Acta Cryst A FOUNDATIONS ADVANCES

ISSN 2053-2733

Absolute refinement of crystal structures by X-ray phase measurements

Sérgio L. Morelhão,[a]* Zohrab G. Amirkhanyan[a] and Cláudio M. R. Remédios[b]

[a]Instituto de Física, Universidade de São Paulo, São Paulo, SP, Brazil, and [b]Faculdade de Física, Universidade Federal Pará, Belém, PA, Brazil. *Correspondence e-mail: morelhao@if.usp.br

Received 16 December 2014
Accepted 5 February 2015

Edited by A. Altomare, Institute of Crystallography - CNR, Bari, Italy

Keywords: single crystals; chirality; invariant phase triplets; X-ray diffraction.

A pair of enantiomer crystals is used to demonstrate how X-ray phase measurements provide reliable information for absolute identification and improvement of atomic model structures. Reliable phase measurements are possible thanks to the existence of intervals of phase values that are clearly distinguishable beyond instrumental effects. Because of the high susceptibility of phase values to structural details, accurate model structures were necessary for succeeding with this demonstration. It shows a route for exploiting physical phase measurements in the crystallography of more complex crystals.

1. Introduction

The methods of X-ray, neutron and electron diffraction are of fundamental importance in crystallography where resolution in determining crystal structures relies primarily on refinement procedures. The collection of large data sets of diffracted intensities and adjustment of parameters in model structures to simulate the experimental intensities are the very basic steps common to all refinement procedures. Apart from these procedures, there are also validation tools necessary in structural biology to avoid serious errors when resolving macromolecular crystals from electron-density maps (Read *et al.*, 2011). Structural resolution in crystallography in the 21st century is therefore limited to structural details producing an unambiguous set of diffracted intensities in atomic models presenting physical and chemical consistency.

Besides intensity measurements, which are measurements of the amplitude of structure factors, physical measurements of structure-factor phases are also possible but only for X-rays (Amirkhanyan *et al.*, 2014). In the early 2000s, bright X-ray sources (synchrotrons) combined with precise multi-axis goniometers created the opportunity of using phase measurements as a physical solution of the phase problem in crystallography (Weckert & Hümmer, 1997; Thorkildsen & Larsen, 1998; Shen *et al.*, 2000; Morelhão & Kycia, 2002; Mo *et al.*, 2002; Soares *et al.*, 2003). This opportunity has been frustrated mainly due to disagreements between the obtained phase values and expected ones in standard samples (Soares *et al.*, 2003; Morelhão, 2003*a*; Shen, 2003). Instrumental effects are a major cause of disagreement. But, as we shall demonstrate, phase values can be highly susceptible to small structural details beyond what is usually accounted for by structural models based on refinement of diffracted intensities. Inaccuracy of theoretical values may also be responsible for disagreements between experimental and expected values.

A turning point in the role of physical phase measurements in X-ray crystallography arises by understanding two facts. (i) There is a window of accuracy for accessing phase values

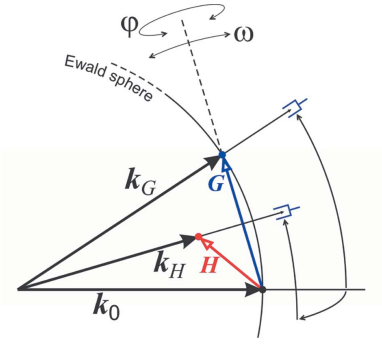

where the measured phases are accurate enough to be used either as a probe of structural features that are inaccessible by standard methods based on refinement procedures (Shen *et al.*, 2006; Morelhão *et al.*, 2011; Amirkhanyan *et al.*, 2014), or as a new structure validation tool in crystallography. (ii) This window depends on the phase value itself. A clear picture is therefore established: practical applications of phase measurements require a good knowledge of the structures in order to obtain theoretical phases very close to the actual phases, which makes it feasible to plan experiments within the window of accuracy.

In this work, we demonstrate how to use theoretical phase values for planning an experiment to inspect features susceptible to changes when designing single crystals. Atomic disorder in one particular group of atoms, a small change in atomic fractional coordinates due to internal stresses and enantiomorphism are some of these features. The emphasis is on the accuracy needed to describe the structure for succeeding in this demonstration, and establishing precedents for a discussion on the realistic perspectives of using physical phase measurements as a new procedure in the crystallography of macromolecular crystals.

2. Principles of phase measurements

Measuring the integrated intensity of one reflection, reflection G, as a function of the excitement of another reflection, reflection H, gives rise to intensity profiles that depend on the invariant phase triplet,

$$\Psi = \delta_H + \delta_{G-H} - \delta_G, \qquad (1)$$

where δ_X is the phase of structure factor, F_X, of reflection X ($X = G$, H and $G - H$). Because of many factors that also affect the intensity profiles, *e.g.* crystalline imperfections, phase measurements have been a low-precision procedure. The exceptions are for Ψ values close to $\pm 90^\circ$. Intensity profiles on each side of these reference values have distinct asymmetries, which provide our window of accuracy.

To illustrate the procedure of planning an experiment based on phase measurements, consider that in a well known structure three invariant phases [equation (1)] with a common δ_G phase were previously selected. Intensity profiles for measuring these invariant phases provide a characteristic pattern of asymmetries, for instance D|C–D|C–C|D as seen in Fig. 1(*a*) where the letter D or C stands for destructive or constructive interference, *i.e.* low- or high-intensity shoulder, respectively. Any structural difference that changes mainly δ_G, without significantly affecting $\delta_H + \delta_{G-H}$, will produce a systematic shift in the Ψ values of all these cases. When the shifts have enough magnitude to cross the $\pm 90^\circ$ values, such a difference in structure is followed by remarkable changes in the pattern of asymmetries. Decreasing or increasing δ_G gives rise to C|D–D|C–D|C or D|C–C|D–C|D patterns, respectively (Figs. 1*b* and 1*c*). It is also possible to exploit structural differences producing changes in $\delta_H + \delta_{G-H}$, and leaving δ_G unchanged. It would provide another pattern of asymmetries, such as C|D–C|D–C|D in Fig. 1(*d*).

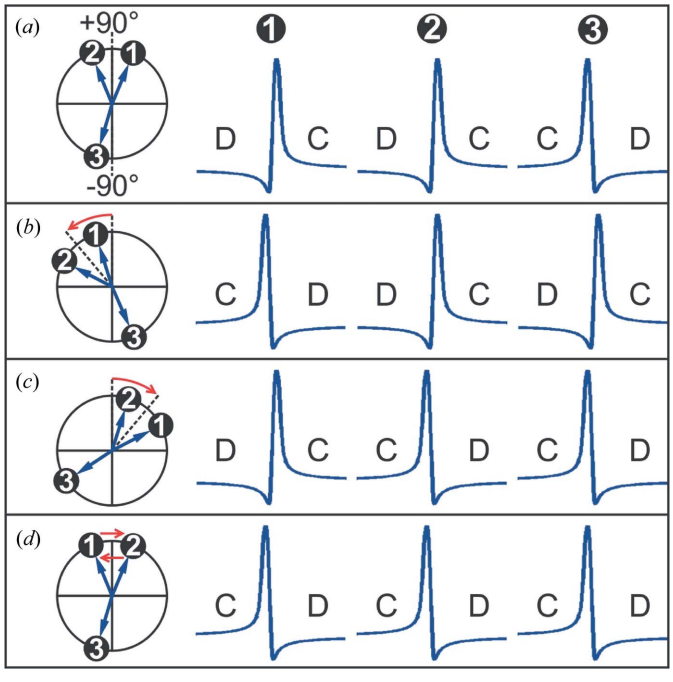

Figure 1
Profile asymmetries as a function of phase shifting. (*a*) Three profiles in a well known structure with invariant phase triplets indicated at the left-hand side. (*b*), (*c*), (*d*) Changes of asymmetries due to phase shifting across the reference values of $\Psi = \pm 90^\circ$. Labels C/D stand, respectively, for the constructive/destructive type of interference giving rise to profile asymmetries.

3. Materials and experimental methods

Single crystals grown from solutions are, in general, well known systems where structural differences are easily introduced by changing the growth environment, for example, a solution of $NH_4H_2PO_4$ (ADP) (Tenzer *et al.*, 1958; Khan & Baur, 1973) with a small concentration of Ni^{2+} and Cl^-. To investigate this system by phase measurements, we choose reflection 400 as the G reflection, the structure-factor phase of which is very susceptible to small rotations and disorder of oxygen sites (Appendix *A*, Fig. 8). On the other hand, a large clockwise rotation of 59.8° around the c axis stands for an enantiomer of this crystalline system in which δ_G has the same value.

Samples were investigated at room temperature, in nearly rectangular $a \times b \times c$ crystals with dimensions of a few millimetres along all axes. Pure and doped samples were grown from supersaturated aqueous solutions with pH 3.9 (1) at 313 K; Ni^{2+}-doped samples were grown in molar solution with 1% of $NiCl_2{\cdot}6H_2O$ and 99% $NH_4H_2PO_4$. The crystal structure is as follows: tetragonal lattice, $a = b = 7.4997\,(4)$, $c = 7.5494\,(12)$ Å, and space group $I\bar{4}2d$ [ICSD (Inorganic Crystal Structure Database) collection code 28154].

X-ray data acquisition was carried out at diffraction station XRD1 of the Brazilian Synchrotron Light Laboratory (LNLS) using a bending magnetic beamline with focusing mirror, two-

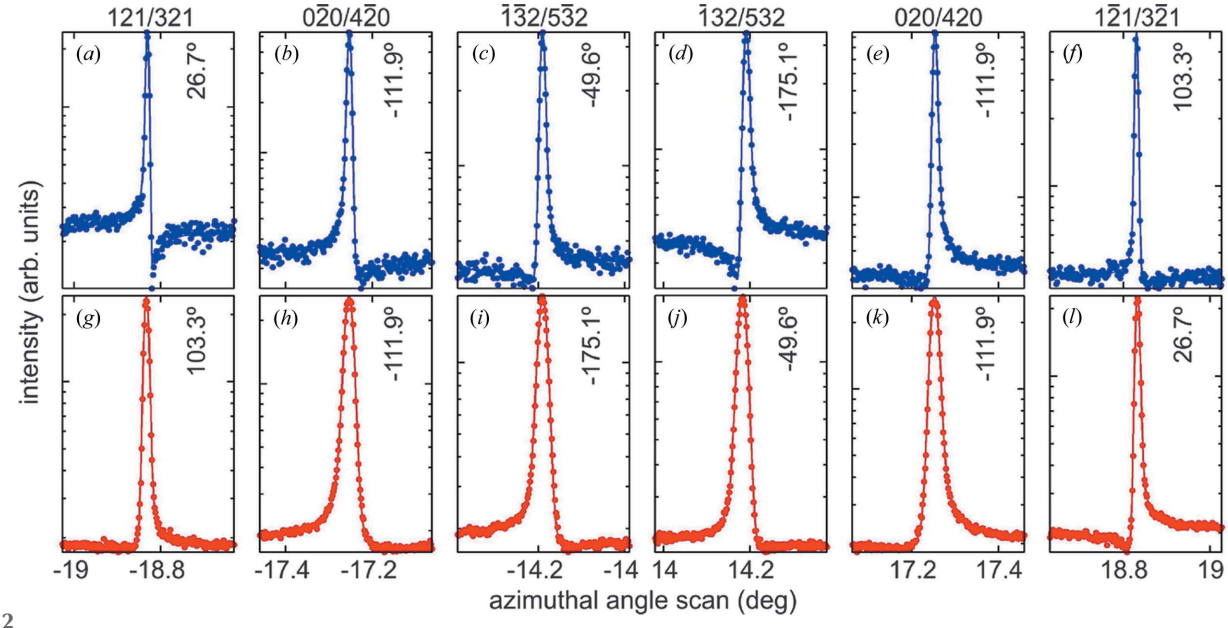

Figure 2
Experimental intensity profiles in crystals grown under different conditions: (*a*)–(*f*) from a supersaturated aqueous solution of $NH_4H_2PO_4$; and (*g*)–(*l*) with 1% addition of $NiCl_2{\cdot}6H_2O$ in molar concentration of solute. Theoretical invariant phase triplets, Ψ values, are shown beside each profile. 400 reflection stands for reflection *G*, while reflections *H* are indicated above the profiles. Synchrotron X-rays of 6.48 keV were used.

bounce Si(111) monochromator with sagittal second crystal and slit screens. X-ray optics were in parallel-beam mode (mirror and sagittal crystal focused at infinity): spectral resolution is 2×10^{-4}, divergences 0.1 mrad and beam size 0.5 mm. Mechanical precision is 0.0002° in the sample rotation stage. A detailed description of the goniometry used can be found elsewhere (Morelhão, 2003*b*).

4. Results and discussion

In the experimental profiles shown in Fig. 2, changes in the pattern of asymmetries are produced by measuring profiles whose invariant phases vary across ±90° in enantiomer crystals (Fig. 3). These profiles correspond to reflections *H* of mixed indexes (odd and even numbers), while those with even numbers exhibit equal invariant phases. For the sake of comparison, profiles in Figs. 2(*c*), 2(*d*) and 2(*b*) can be taken as those in Fig. 1(*a*), while profiles in Figs. 2(*i*), 2(*j*) and 2(*h*) as

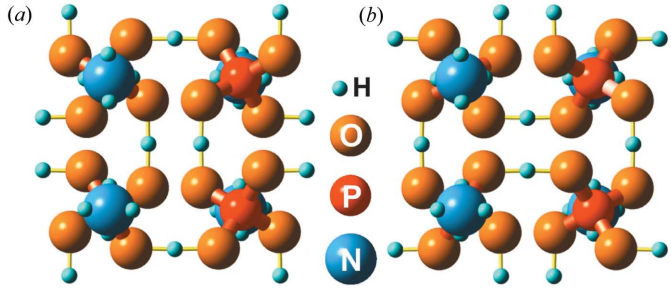

Figure 3
Enantiomer crystals of $NH_4H_2PO_4$. Space group $I\bar{4}2d$, fractional coordinates of O atoms: (*a*) $x = 0.1466$, $y = 0.0843$ and $z = 0.1151$; (*b*) $x = 0.1466$, $y = -0.0843$ and $z = 0.1151$. Top view from the *c* axis. Atom sizes are illustrative.

those in Fig. 1(*d*). Both sets of profiles exhibit asymmetry patterns changing from D|C–D|C–C|D to C|D–C|D–C|D, as illustrated.

More information about the growth mechanism of this system is available from the data set. Profile broadening and smoothing of asymmetries (Figs. 2*g*–2*l*) indicate an increase of mosaicity and shortening of lattice coherence length. In azimuthal scanning, peak positions are very sensitive to unit-cell parameters (Freitas *et al.*, 2007), implying that average strains in the sample are smaller than 10^{-4} within the obtained error bar of ±0.002° in peak position determination (Appendix *A*, Table 2). Moreover, based on the high resolution of phase δ_G to features reported in similar systems, such as internal stresses and disordering of O atoms (Morelhão *et al.*, 2011; Amirkhanyan *et al.*, 2014), the observed pattern of asymmetries shows no evidence of such features. The role of the foreign ions in solution seems to be restricted to the growth front, complicating the crystal growth and inducing the enantiomorph form.

Away from absorption edges, account of corrections due to atomic resonances in standard procedures of intensity data refinement is optional, since the improvement in the reliability factor owing to these corrections can be very small. In this experiment, the nearest absorption edge, which is for P atoms, is more than 4 keV below the X-ray energy used of 6.48 keV. However, in phase measurements, the situation is completely different. It is no longer a question of improving the fit between the simulated and experimental data. By neglecting atomic resonances in this experiment, the observed pattern of asymmetries is irreproducible. For instance, the C|D–C|D–D|C–D|C–D|C–C|D pattern formed by the sequence of profiles in Figs. 2(*a*)–2(*f*) would be C|D–C|D–C|D–D|C–D|C–D|C without resonance

Table 1
Phase triplets Ψ and respective profile asymmetries (Asy.), accounting for scattering by ions or neutral atoms, and resonance (Res.) or no resonance (No res.) corrections (Appendix *A*).

Experimental profiles are shown in Figs. 2(*a*)–2(*f*).

	Ions				Neutral atoms			
	Res.		No res.		Res.		No res.	
Fig. 2	Ψ (°)	Asy.	Ψ (°)	Asy.	Ψ (°)	Asy.	Ψ (°)	Asy.
(*a*)	26.7	C|D	−36.3	C|D	99.7	D|C	135.9	D|C
(*b*)	−111.9	C|D	180	C|D	−31.6	D|C	0.0	D|C
(*c*)	−49.6	D|C	−116.3	C|D	27.4	D|C	60.0	D|C
(*d*)	−175.6	D|C	116.3	D|C	−90.9	C|D	−60	C|D
(*e*)	−111.9	D|C	180	D|C	−31.6	C|D	0.0	C|D
(*f*)	103.3	C|D	36.3	D|C	−168.1	C|D	−135.9	C|D

corrections, as indicated in Table 1 (columns under the label 'Ions').

A similar situation occurs with respect to ionic charges. More than just improving the reliability factor when adjusting the intensity data of individual reflections, using atomic scattering factors for O^{2-}, N^{3-} and P^{5+} ions was needed to obtain $\Psi = -111.9^\circ$, which is a value compatible with the profile asymmetries in Figs. 2(*b*), 2(*e*), 2(*h*) and 2(*k*). Otherwise, scattering factors for neutral atoms, including H atoms, would lead to $\Psi = -31.6^\circ$ (Table 1, columns under the label 'Neutral atoms') and profiles with opposite asymmetries to the measured ones. Another detail in agreement with scattering factors for ions is the asymmetric aspect of profiles in Figs. 2(*a*), 2(*f*), 2(*g*) and 2(*l*). The closer Ψ is to the 90° value, the less asymmetry the profile should exhibit. Hence, the profiles with $\Psi = 26.7^\circ$ are expected to be more asymmetric than the other ones with $\Psi = 103.3^\circ$, as observed.

Phase measurements provide a new horizon to be explored in crystallography, and it is much simpler than initially supposed. Rather than attempting to extract phase values from profile asymmetries with the purpose of using them to improve the reliability of refinement procedures, just collecting and comparing patterns of asymmetries gives enough information for checking the completeness of a determined structure. The difficulty, however, lies in selecting appropriate profiles for measurements. Accurate model structures accounting for feasible differences in fractional coordinates, bonding angles, ionic charges and atomic disorder are required. When models are available, a general strategy for finding measurable phase triplets is graphically represented in Fig. 4. In the case of enantiomorph structures, a weak Bragg reflection with constant phase, $\Delta\delta = 0$, was chosen in Fig. 4(*a*), and major phase triplets giving rise to inversion of profile asymmetries are then identified in Fig. 4(*b*).

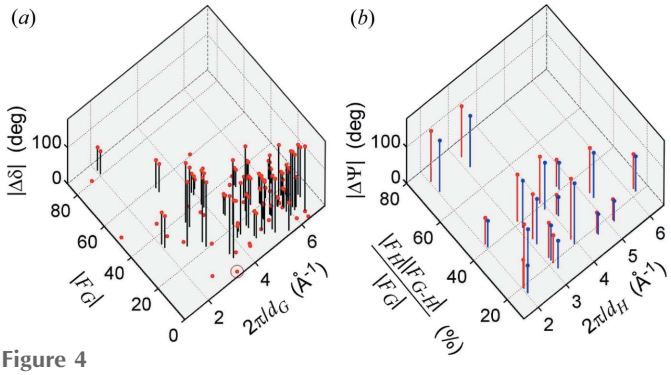

Figure 4
General strategy for finding measurable phase triplets with enhanced accuracy with respect to the difference in structure of crystals. (*a*) Mapping of variation in Bragg reflection phases; and (*b*) phase triplets shifting across ±90° for a chosen reflection *G* in (*a*), marked with a circle. $d_{G,H}$ is the interplanar distance of Bragg planes.

By choosing a very weak reflection *G*, instrumental effects related to sample shape, crystallinity and diffraction geometry are minimized. The influence of the non-phase-carrying term *Aufhellung* becomes very small, as well as of the high-order terms of dynamical coupling among diffracted waves; weak reflections have larger *Pendellösung* length, which minimizes the influence of these high-order terms (Thorkildsen & Larsen, 1998). In the diffraction geometry used where the *G* reflection is a symmetrical Bragg reflection, the instrumental effects are not able to compromise the observed asymmetries between the left and right tails of the intensity profiles. Hence, a direct correlation between C|D or D|C asymmetry and phase triplet Ψ has been possible. In any other diffraction geometry, it would be wise to check, for example, *via* dynamic simulation (Weckert & Hümmer, 1997), if this direct correlation is still valid for weak reflections *G*.

The mechanism by which phase measurements solve the chirality is independent of anomalous scatterers. In all cases where only the phases of reflections *H* and $G - H$ change with chirality, the phase triplets are $\Psi_\pm = \pm|\delta_H + \delta_{G-H}| - \delta_G$ in the absence of atomic resonances. When δ_G is too close to 0 or 180°, both Ψ_+ and Ψ_- will be in the same half of the trigonometric circle with respect to the reference values ±90°. Then, the profiles of both enantiomers will have a similar appearance (asymmetric aspect), but one of them will be more asymmetric than the other. Solving chirality in this case requires a more careful experiment with samples of the same shape and crystallinity, since these parameters may also impact the level of asymmetry of a given profile. On the other hand, when δ_G is close to ±90°, the profiles show opposite asymmetries, allowing a much more reliable determination of chirality as exploited in this work. Atomic resonances affect the phase values of individual reflections and so must be taken

Table 2
Theoretical values of $F_H F_{G-H} = |F_H F_{G-H}| \exp[i(\delta_H + \delta_{G-H})]$ for multi-beam diffraction peaks observed in Fig. 6.

G stands for the 400 reflection, $|F_G| = 2.14$ and $\delta_G = 117.6°$. (−/+) indicate enantiomers, ADP− (Fig. 3*b*) and ADP+ (Fig. 3*a*) crystals. Experimental peak positions φ_0, and widths FWHM, were obtained by a line profile function described elsewhere (Freitas *et al.*, 2007).

	$\lvert F_H F_{G-H}\rvert$		$\delta_H + \delta_{G-H}$ (°)		Peak position, φ_0 (°)		FWHM (″)	
H	(−)	(+)	(−)	(+)	(−)	(+)	(−)	(+)
12̄1/32̄1	1294	1116	144.3	−139.1	−18.830 (±1)	−18.832 (±2)	32	45
02̄0/42̄0	2730	2730	5.7	5.7	−17.253 (±1)	−17.252 (±2)	37	77
1̄32̄/53̄2̄	2092	1937	68.0	−57.5	−14.191 (±1)	−14.187 (±2)	46	83
1̄32̄/532	1937	2092	−57.5	68.0	14.191 (±1)	14.187 (±2)	53	88
020/420	2730	2730	5.7	5.7	17.253 (±1)	17.252 (±2)	37	75
12̄1/32̄1	1116	1294	−139.1	144.3	18.830 (±1)	18.832 (±2)	32	41

into account when planning an experiment to solve chirality by using this ideal condition of profiles with opposite asymmetries.

5. Conclusions

The use of phase measurements in crystals with large unit cells is a procedure that requires an investment of time for accumulating the necessary knowledge on structural features and their influences on phase values. From the example presented here of a small molecule, even resonance terms away from absorption edges and ionic charges were important for properly evaluating the experimental patterns of profile asymmetries. In large molecules, it is necessary to learn how precisely we must describe all subunits of a molecule before being able to use phase measurements for improving structural resolution.

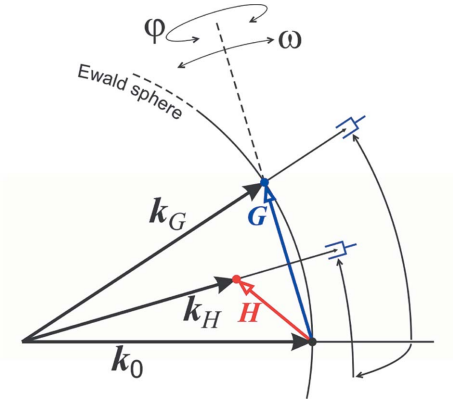

Figure 5
Diffraction geometry for physical phase measurements. Integrated intensity of one reflection, *G* or *H*, as a function of excitement of another, *H* or *G*. Enhanced contribution of invariant phase triplet on intensity profiles is obtained by measuring the weaker reflection.

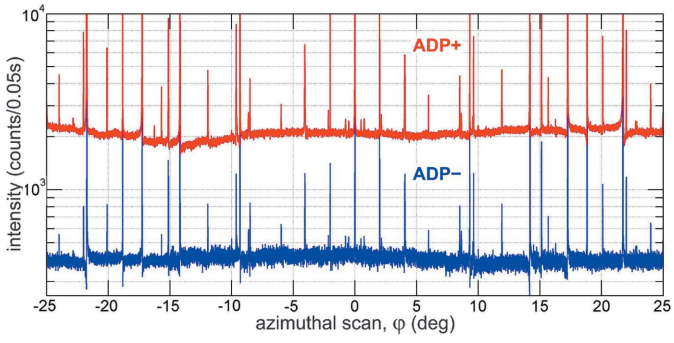

Figure 6
Azimuthal scans of the 400 reflection in enantiomer crystals of ADP. Synchrotron X-rays of 6.48 keV, σ polarization. Reference direction ($\varphi = 0$): *c* axis in the incident plane pointing upstream. Sense of rotation: counterclockwise with the diffraction vector pointing to the observer.

APPENDIX *A*

A1. Diffraction geometry

Possible diffraction geometries for physical phase measurements are depicted in Fig. 5. In this work, we measured the intensity of reflection *G* while exciting reflection *H* by rotating the sample around the φ axis (Morelhão, 2003*b*). Wide azimuthal scans (φ scans) of both samples are shown in Fig. 6.

A2. Choice of reflection

The phase of the 400 reflection is very susceptible to disorder and displacement of O atoms, as illustrated in Fig. 7 and quantitatively analysed in Fig. 8. But it is invariant in this pair of enantiomers.

Because of crystal symmetry and choice of the 400 reflection, most profiles stand for two coincident three-beam diffraction cases, *i.e.* two reflections *H* are simultaneously excited as indicated above each profile in Fig. 2 as well as in the first column of Table 2. Although each one of these three-

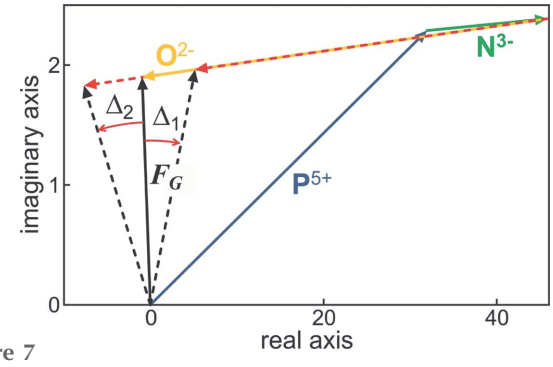

Figure 7
Argand diagram for structure factor F_G of reflection 400 in an ADP crystal. Contributions of each chemical species, N^{3-}, P^{5+} and O^{2-}, are shown separately. Either disorder of oxygen sites or rotation of PO_4 units can give rise to phase shifts, but in opposite direction: disorder $\Rightarrow \Delta_1$ and rotation $\Rightarrow \Delta_2$.

Table 3
Cromer–Mann coefficients a_n and b_n, and resonance correction terms f' and f'', for calculating atomic scattering factors *via* equation (2).

Ion	a_0	a_1	a_2	a_3	a_4	b_1	b_2	b_3	b_4	f'	f''
N	−11.52900	12.21260	3.132200	2.012500	1.166300	0.005700	9.893300	28.99750	0.582600	0.0452	0.0286
N^{3-}	−3.000230	4.142775	4.416557	0.794703	3.650171	0.042821	33.75266	0.995284	11.26764	0.0452	0.0286
P	1.114900	6.434500	4.179100	1.780000	1.490800	1.906700	27.15700	0.526000	68.16450	0.3563	0.6486
P^{5+}	1.105043	1.695751	0.177933	0.549250	6.462256	0.503103	10.48811	12.97966	1.871460	0.3563	0.6486
O	0.250800	3.048500	2.286800	1.546300	0.867000	13.277100	5.701100	0.323900	32.90890	0.0704	0.0506
O^{2-}	0.456290	0.562170	4.998626	2.565331	1.415686	33.47635	9.042666	32.91774	0.432043	0.0704	0.0506
H	0.003038	0.493002	0.322912	0.140191	0.040810	10.51090	26.12570	3.142360	57.79970	0.0	0.0

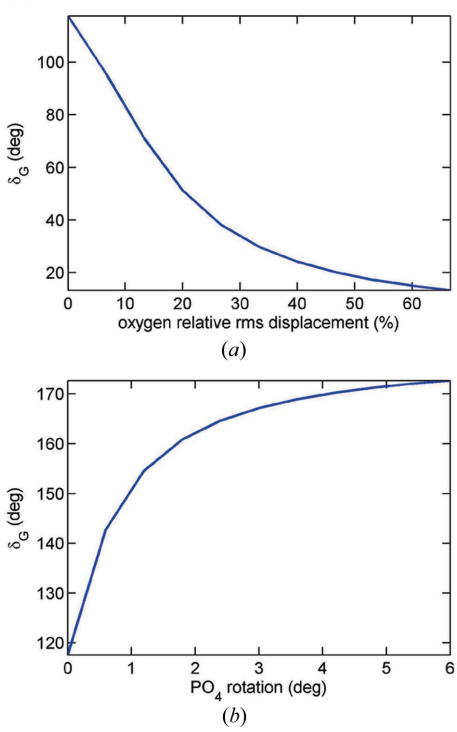

Figure 8
Phase of structure factor F_G, of the 400 reflection, as a function of (*a*) relative root-mean-square displacement of O atoms above thermal vibrations, and (*b*) counterclockwise rotation of PO_4 units around the *c* axis. $\delta_G = 117.6°$ when all atoms have nearly the same Debye–Waller factor and O atoms have fractional coordinates (0.1466, 0.0843, 0.1151).

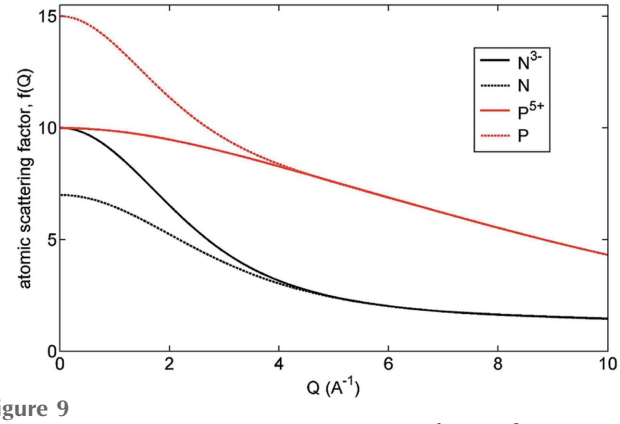

Figure 9
X-ray non-resonant atomic scattering factors of N^{3-} and P^{5+} ions used for calculating structure factors. For the sake of comparison, values for neutral atoms are also shown.

beam diffraction cases may have differences in strength, they carry the same invariant phase and asymmetric aspect, as explained elsewhere (Weckert & Hümmer, 1997; Amirkhanyan *et al.*, 2014).

A3. Atomic scattering factors

Atomic scattering factors were estimated by

$$f(Q,\mathcal{E}) = a_0 + \sum_{n=1}^{4} a_n \exp\left[-b_n\left(\frac{Q}{4\pi}\right)^2\right] + f'(\mathcal{E}) + if''(\mathcal{E}), \quad (2)$$

with parameters a_n, b_n, f' and f'' as given in Table 3 for X-rays of energy $\mathcal{E} = 6.48$ keV. $Q = 2\pi/d$ where d is the interplanar distance of Bragg planes. For N^{3-} and P^{5+} ions, a_n and b_n were obtained by a similar procedure previously used (Amirkhanyan *et al.*, 2014). The atomic scattering factors of these ions are compared to those for neutral atoms in Fig. 9.

Acknowledgements

This work was supported by FAPESP (grant Nos. 2012/01367-2 and 2014/08819-1), CNPq (grant No. 306982/2012-9) and LNLS.

References

Amirkhanyan, Z. G., Remédios, C. M. R., Mascarenhas, Y. P. & Morelhão, S. L. (2014). *J. Appl. Cryst.* **47**, 160–165.
Freitas, R. O., Lamas, T. E., Quivy, A. A. & Morelhão, S. L. (2007). *Phys. Status Solidi A*, **204**, 2548–2554.
Khan, A. A. & Baur, W. H. (1973). *Acta Cryst.* B**29**, 2721–2726.
Mo, F., Mathiesen, R. H., Alzari, P. M., Lescar, J. & Rasmussen, B. (2002). *Acta Cryst.* D**58**, 1780–1786.
Morelhão, S. L. (2003*a*). *Acta Cryst.* A**59**, 470–480.
Morelhão, S. L. (2003*b*). *J. Synchrotron Rad.* **10**, 236–241.
Morelhão, S. L. & Kycia, S. (2002). *Phys. Rev. Lett.* **89**, 015501.
Morelhão, S. L., Remédios, C. M. R., Freitas, R. O. & dos Santos, A. O. (2011). *J. Appl. Cryst.* **44**, 93–101.
Read, R. J. *et al.* (2011). *Structure*, **19**, 1395–1412.
Shen, Q. (2003). *Acta Cryst.* A**59**, 335–340.
Shen, Q., Elfimov, I. S., Fanwick, P., Tokura, Y., Kimura, T., Finkelstein, K., Colella, R. & Sawatzky, G. A. (2006). *Phys. Rev. Lett.* **96**, 246405.
Shen, Q., Kycia, S. & Dobrianov, I. (2000). *Acta Cryst.* A**56**, 264–267.
Soares, A. S., Caspar, D. L. D., Weckert, E., Héroux, A., Hölzer, K., Schroer, K., Zellner, J., Schneider, D., Nolan, W. & Sweet, R. M. (2003). *Acta Cryst.* D**59**, 1716–1724.
Tenzer, L., Frazer, B. C. & Pepinsky, R. (1958). *Acta Cryst.* **11**, 505–509.
Thorkildsen, G. & Larsen, H. B. (1998). *Acta Cryst.* A**54**, 120–128.
Weckert, E. & Hümmer, K. (1997). *Acta Cryst.* A**53**, 108–143.